Hindawi
Advances in Materials Science and Engineering
Volume 2019, Article ID 8135253, 9 pages
https://doi.org/10.1155/2019/8135253

Research Article

Effect of Rare Earth Ce on the Microstructure and Mechanical Properties of 34CrNiMo6 Steel for Wind Turbine Main Shaft

Yanming Ge and Kehong Wang

School of Materials Science and Engineering, Nanjing University of Science and Technology, Nanjing 210094, China

Correspondence should be addressed to Kehong Wang; wkh1602@126.com

Received 3 January 2019; Accepted 4 March 2019; Published 1 April 2019

Academic Editor: Zhonghua Yao

The effect of rare earth Ce on mechanical properties is studied by investigating the precipitates evolution during heat treatment of 34CrNiMo6 steel. Five different rare earth Ce contents are carried out with the same holding time 3 hours. Then, the mechanical properties of 34CrNiMo6 steel are obtained under steady state conditions and impact conditions, respectively. The strength decreases while the elongation after breakage increases with the rare earth Ce content increasing. The impact absorbing energy at 20°C and −40°C increases with the rare earth Ce content increasing. Based on the experimental results, the recommended rare earth Ce content is 0.05 wt.%. The differences in mechanical properties among the different rare earth Ce contents may be the nucleation rate and growth of precipitates under different conditions. The spherification degree of cementite is more complete with rare earth Ce content, resulting in the decrease of mechanical properties and improvement of ductility.

1. Introduction

The modern development of commercial wind power industries started in the 1970s in the United States before spreading to Europe where Denmark and Germany became significant champions of the technology [1]. The focus of growth has shifted to Asia and particularly to China, where there has been massive development of wind power during the past decade. So the wind energy is one of the fastest growing sources of electricity, and it is capable of providing power in most parts of the world nowadays [2]. According to the estimation of International Energy Agency (IEA), the annual wind-generated electricity of the world will reach 1282 TWh by 2020. By 2030, the annual wind-generated electricity will reach 2182 TWh [3]. That requires the wind turbines having the higher safety and reliability, with the power of wind turbines increasing from kilo-watt-class to million-watt-class [4]. That is to say, the mechanical properties of material used for making main bearing should meet the related demands [5]. 34CrNiMo6 steel is one kind of heat-treated low alloy steel with high hardenability and strength, which contains nickel, chromium, and molybdenum [6]. Moreover, 34CrNiMo6 steel has very good toughness properties with Charpy V-notch at a very low temperature. Hence, 34CrNiMo6 steel is widely used for making the wind turbine main shaft [7]. In the actual production process, a typical heat treatment for this steel involves two stages, quenching and tempering [8]. The 34CrNiMo6 steel could obtain high strength after quenching to a full martensitic microstructure, while the ductility and toughness can be improved by the tempering process. Popescu et al. [9] studied on the parameters of bulk tempering process on the hardenability and temperability of 34CrNiMo6 steel. The experiment investigated the correlation between the hardness achieved after high tempering on products and their equivalent diameter and the heat and time parameters of tempering. Cochet et al. [10] investigated the heat treatment parameters of 34CrNiMo6 steel used for shackles. The results firstly provided a validation of the input data and the prediction of the phase volume fractions and the resulting hardness, which showed that the proposed approach could yield a very good representation of the material properties. The results show that the heat treatment method could improve the mechanical properties significantly via changing the

nucleation rate and growth rate of austenite. However, there are very few researches about specific effect of rare earth Ce on microstructure and mechanical properties of 34CrNiMo6 steel during tempering process.

One of the most important things for a production company is to provide qualified products, which should meet the certification standard. As the key part of wind turbine, the main shaft undertakes various loads transmitted by the hub, it performs heavy duty operations and carries both dynamic and stochastic loads, and its failure could result in major catastrophe and lead to significant economic losses. The fault statistics of the wind turbine in Figure 1 shows that the outages caused by the main shaft failure account for less than 0.1% (marked in blue), but its downtime accounts for a very large share, about 24.8% (marked in orange) [11]. So it is necessary to investigate the mechanical properties of 34CrNiMo6 steel for wind turbine main shaft after the heat treatment.

The objective of this paper is to investigate the microstructure evolution and mechanical properties of 34CrNiMo6 steel by adopting different rare earth Ce contents. That could help to understand and optimize the heat treatment process parameters that affect the microstructures, which could determine the final mechanical properties of 34CrNiMo6 steel for wind turbine main shaft. Firstly, we used five different rare earth Ce contents before heat treatment process. Then, the mechanical property tests of tensile strength, yield strength, elongation after breakage, and impact absorbing energy under the different conditions were carried out, respectively. To get a better understanding of the influencing mechanism of rare earth Ce on the microstructures evolution of 34CrNiMo6 steel, the metallographic investigations from the optical microscope (OM), scanning electron microscope (SEM), and transmission electron microscope (TEM) were presented, respectively.

2. Materials and Methods

The material used on the present study is the heat-treated low-alloy 34CrNiMo6 steel. In this experiment, we designed five different rare earth Ce contents to investigate the effect of rare earth Ce content on microstructure and mechanical properties 34CrNiMo6 steel, and the chemical compositions of the material are listed in Table 1. Ce was added in the form of Fe-10Ce master alloy, and the Fe-10Ce master alloy ingots were prepared by melting pure Fe and pure Ce with a purity of 99.9% in a vacuum melting frunace.

The heat treatment process for 34CrNiMo6 steel involves two stages, quenching and high-temperature tempering (QT). Again, the steel could obtain high strength by quenching and improve toughness by the tempering process. Table 2 illustrates the mechanical properties required according to certification of 34CrNiMo6 steel for wind turbine main shaft and BS EN 10083-3: 2006.

According to actual measurement, the fracture position occurred in the variable diameter section of the inner diameter of the main shaft. The schematic diagram and numerical simulation of the wind turbine main shaft are shown in Figure 2. The image of fracture surface is shown on the right. The definition of the linear elastic material constitutive model was adopted, and the stress values were analyzed under the rated load condition and the impact condition, respectively. In order to obtain a reasonable stress distribution of the main shaft, the wind loads were obtained by aerodynamics analysis using a FAST procedure [12]. According to the finite element method simulation, we can know that the positions of the maximum internal stress of main shaft are always located at the center of the variable section both under steady-state conditions and impact conditions. So the specimens used in this experiment were taken from the variable diameter section.

The heat treatments of 34CrNiMo6 steel consist of several steps, each of them having a specific purpose. Specifically, the tempering process is to reduce the brittleness, relieve the internal stress, and obtain relatively good microstructures. The tempering process includes heating the martensitic steel to the temperature below the lower transformation temperature (A1), holding for specified time period and then cool down to room temperature, which could make 34CrNiMo6 steel achieve the combination of mechanical properties [13]. The most important process parameters during tempering are tempering temperature, holding time and the steel chemical composition [14]. The tempering temperature can be identified according to the superficial color during heating and the holding time could be determined by the product size, respectively. Generally, the larger product sizes, the more the time for heating to the tempering temperature. On the other hand, the temperature and holding time are interdependent parameters in the tempering process. So it could obtain a range of mechanical properties by combination of the tempering temperature and holding time, as shown in Figure 3. The heat treatment condition used in this study is as shown in Table 3.

These wind turbine main shaft needs to exhibit high levels of strength and toughness over an extended period. Accordingly, the related tests were carried out to verify the mechanical properties according to standard specifications. The mechanics performance testing contains tensile strength, yield strength, elongation after breakage, and impact absorbing energy test. Strength is one of the main mechanical properties of metals and alloys, which is defined as the amount of stress that a material can withstand while being tensile or compressed before failing. Toughness is defined as the ability of the metal to resist fracture by absorbing impact energy and through plastic deformation. Fracture toughness is used to characterize toughness. An impact test is used to give an indication of fracture toughness through measuring the resistance of the material to impact load without fracture [15], which can be used as a tool to evaluate the ductile-brittle transition temperature. In addition, hardness is also a very important parameter of material, which is a measure of the resistance to localized plastic deformation induced by either mechanical indentation or abrasion.

The tensile test is based on the Standard ASTM E8, the specimen is taken from the 1/4 position of circular cross section of the 34CrNoMo6 diameter, whose original diameter is 10 mm, original standard distance is 50 mm, and total length is 120 mm, as shown in Figure 4(a). The tensile test was carried out via the hydraulic universal tester WAW-300B, and the load rate was set as 1 mm/min. The samples

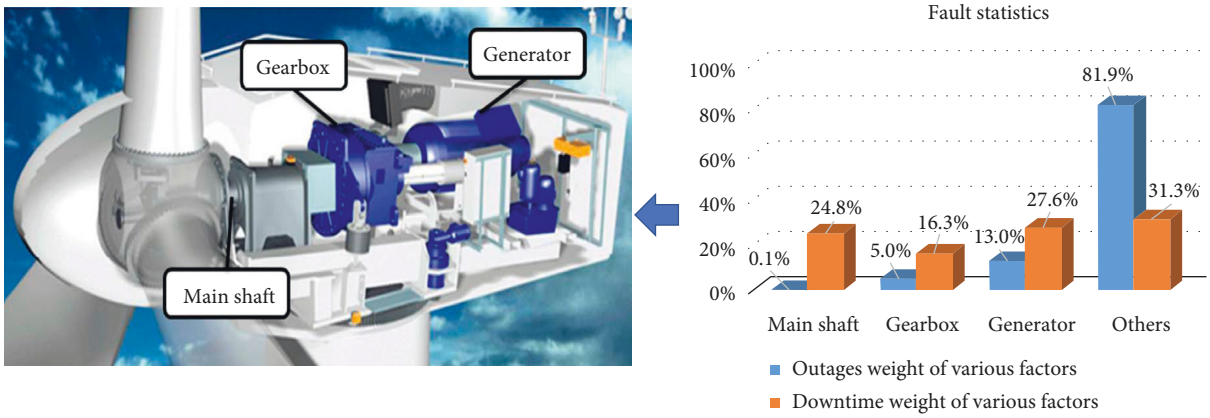

Figure 1: Outages and downtime weights of wind turbine faults.

Table 1: Chemical compositions of 34CrNiMo6 steel (mass fraction, %).

Element	Ce	C	Si	Mn	P	S	Cr	Mo	Ni
Standard value BS EN 10083-3: 2006	—	0.30–0.38	0.40	0.50–0.80	0.025	0.035	1.30–1.70	0.15–0.30	1.30–1.70
1#	0	0.35	0.23	0.76	0.011	0.001	1.58	0.22	1.53
2#	0.01	0.32	0.22	0.76	0.011	0.001	1.59	0.23	1.54
3#	0.025	0.33	0.24	0.77	0.011	0.001	1.56	0.23	1.54
4#	0.05	0.34	0.21	0.77	0.011	0.001	1.55	0.24	1.55
5#	0.11	0.33	0.24	0.75	0.011	0.001	1.57	0.23	1.54

Table 2: Mechanical properties of 34CrNiMo6 steel for wind turbine main shaft.

Test items	Tensile strength R_m (MPa)	Yield strength R_e (MPa)	Elongation A (%)	Impact absorbing energy AKV (J)
Standard value BS EN 10083-3: 2006	1100–1300	≥900	≥10	≥100 (+20°C) ≥90 (−40°C)

were tested 3 times, and the test results were averaged for each group of samples.

According to the Standard ASTM A370-2013a, the impact tests are carried out to measure impact absorbing energy. The specimen is shaped as V-type taking from the 1/4 position of circular cross section of the 34CrNoMo6 diameter, whose total length is 50 mm. The height and width of the section both are 10 mm, the notch angle is $45 \pm 2^{\circ}$, and the height of the notch at the bottom is 8 mm, as shown in Figure 4(b). The impact tests were carried out by the impact testing machine ZBC2302. The samples were tested 3 times, and for each group of samples, the test results were averaged.

The hardness test is based on the Standard ASTM E18-2015. All the sample surfaces were ground and polished before hardness tests. After placing the samples in the hardness testing machine, a load with 150 kgf was applied on the samples. After the load was removed, the Rockwell hardness C (HRC) could be calculated out.

3. Results and Discussion

3.1. Effect on Tensile Properties and Surface Hardness. The evolutions of strength and elongation and the hardening curves of 34CrNiMo6 steels in tensile tests with different rare earth Ce contents are shown in Figures 5 and 6, respectively.

As shown in Figure 5(a), both the tensile strength and yield strength decrease with the rare earth Ce content increasing. In contrast, the elongation after breakage increases with rare earth Ce content increasing before 0.05 wt.%, while remains almost stable from 0.05 wt.% to 0.1 wt.%. According to the certification standard in Table 2, we could know that the integrated mechanical properties of 34CrNiMo6 steel meet the demands when the rare earth Ce content is below 0.05 wt.%. The tensile strength is lower than the required value when the rare earth Ce content is 0.1 wt.%. From the above, the rare earth Ce content is recommended no more than 0.05 wt.%. As shown in Figure 6, no matter whether Ce is added or not, the tensile strength of 34CrNiMo6 is very good, and the two stress-strain curves (Ce = 0% and Ce = 0.05%) both have clear upper yield points. Moreover, the ductility of the 34CrNiMo6 steel is increased when 0.05 wt.% Ce is added into the 34CrNiMo6 steel.

The evolution of surface hardness with the Ce content is shown in Figure 7. The Rockwell hardness C decreases with Ce content increasing before 0.05 wt.%, while remains almost stable from 0.05 wt.% to 0.1 wt.%. Huang et al. [16] studied on strength and ductility of 34CrNiMo6 steel produced by laser solid forming (LSF) and found that the hardness of the LSF + QT (quenching-tempering) sample was 310HV, i.e., 31 HRC. Through comparison, we could

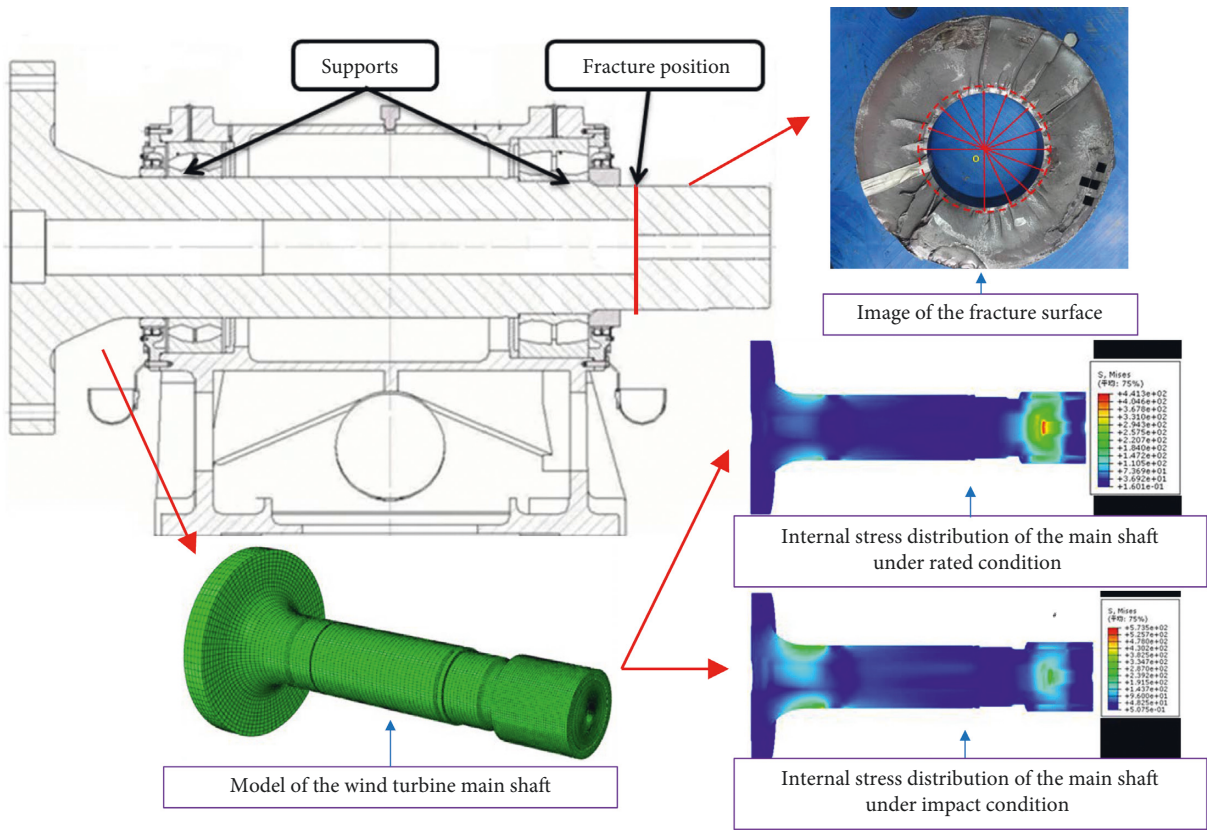

Figure 2: Numerical simulations of the wind turbine main shaft.

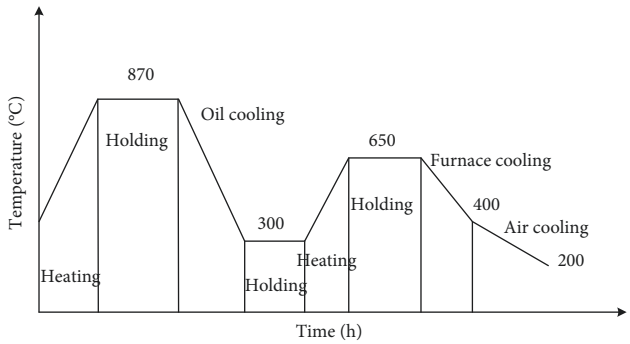

Figure 3: The flow chart of the main shaft heat treatment process.

Table 3: Heat treatment conditions.

Austenitising temperature (°C)	Tempering temperature (°C)	Holding time (h)
870	650	3

indicate that the addition of rare earth Ce would reduce the hardness of 34CrNiMo6 steel to a certain extent, but the reduced hardness value was still at a reasonable level and would meet the related requirements.

3.2. Effect on Impact Energy Absorbed. The evolutions of the impact absorbing energy with the rare earth Ce content under different temperatures are shown in Figure 8.

As shown in Figure 8, the impact absorbing energy increases with the rare earth Ce content increasing, and reaches the peak value when then testing temperature is 20°C. Then, the impact absorbing energy decreases from 0.05 wt.% to 0.1 wt.%. According to the specification design, the impact absorbing energy meets the related requirements when rare earth Ce content is over 0.025 wt.%. In contrast, the impact absorbing energy increases monotonously with rare earth Ce content increasing when the testing temperature is −40°C, as shown in Figure 8. According to the specification design, the impact absorbing energy meets the related requirements when rare earth Ce content is over 0.01 wt.%.

According to the previous mechanical performance test results and related certification standard, it is highly recommended that the rare earth Ce content should be from 0.025 wt.% to 0.05 wt.%.

3.3. Effect on Microstructures and Fracture Morphologies. The metallographs of 34CrNiMo6 steel after quenched and QT from OM are shown in Figure 9, respectively.

As previously mentioned, the 34CrNiMo6 steel could obtain high strength by quenching to a full martensitic microstructure. According to the major morphologies, martensites could be divided into two main types, martensite lath and plate martensite. In this paper, the morphology of martensites consists mostly of dislocated martensite laths, as shown in the Figure 9(a).

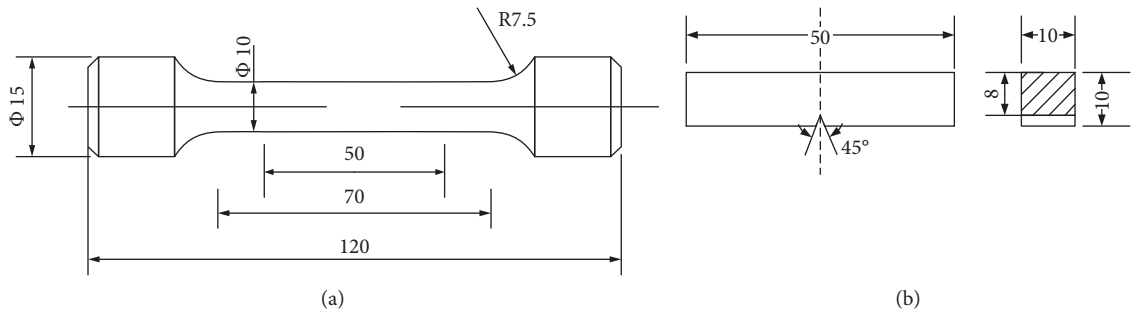

Figure 4: Schematic diagrams of the specimens (mm): (a) tensile test specimen, (b) impact test specimen.

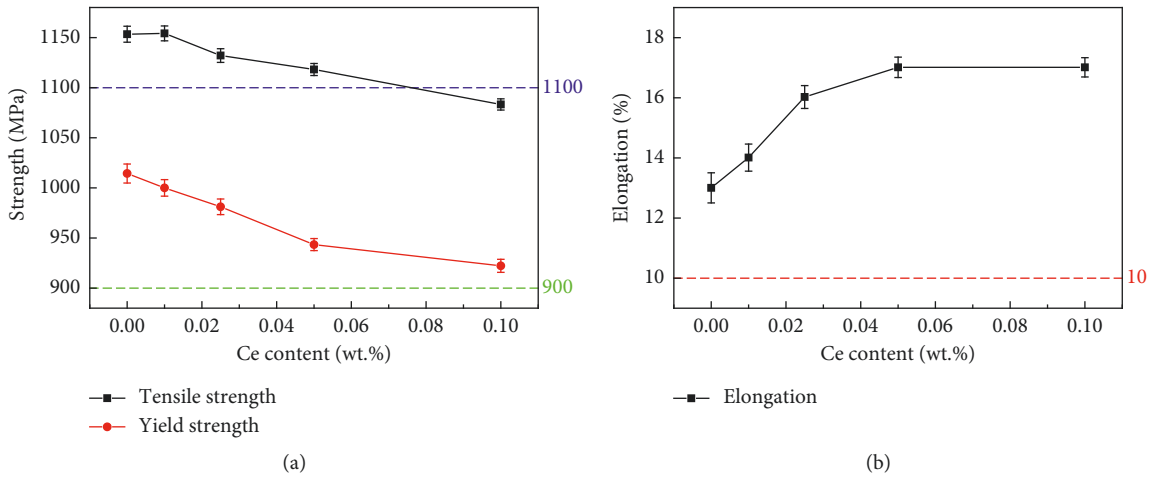

Figure 5: The evolutions of strengths and elongations with the rare earth Ce content: (a) tensile strength and yield strength; (b) elongation after breakage.

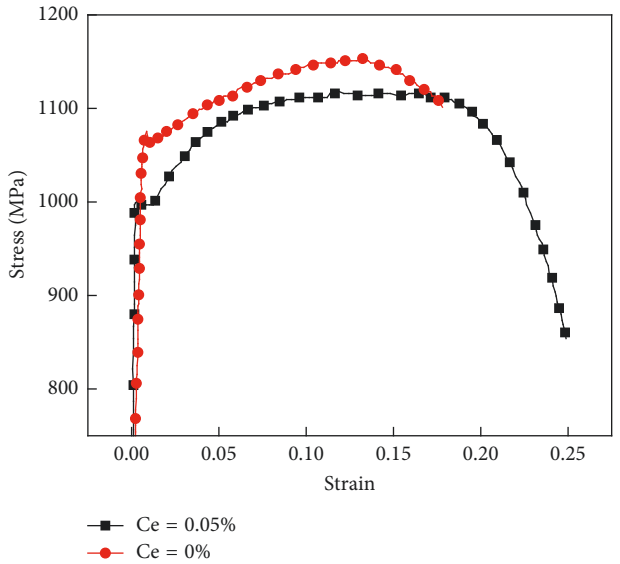

Figure 6: Hardening curves in tensile tests with the content of rare earth Ce.

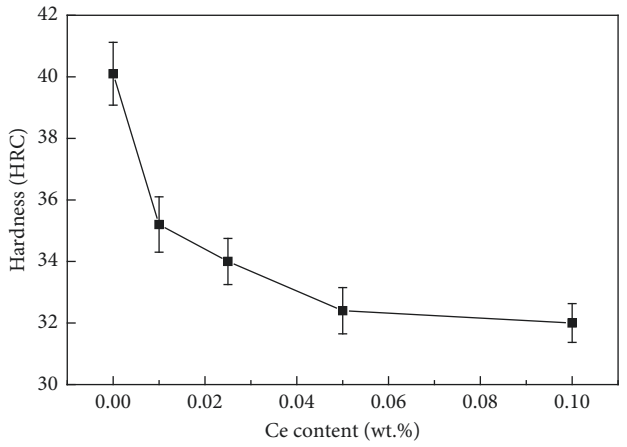

Figure 7: The evolutions of hardness with the rare earth Ce content.

After comparing the metallographs of 34CrNiMo6 steel from OM under different rare earth Ce contents, the investigation of the samples point out there are few differences in the microstructures among them. The microstructures after tempering from OM is shown Figure 9(b). During tempering process, the martensites decompose and then transform to ferrite and metastable phase of ε-carbide. The cementite will be formed later and eventually the ferrite matrix recrystallizes. [17] Most of the recrystallized ferrite has a chaotic ordering and interlocking structure that

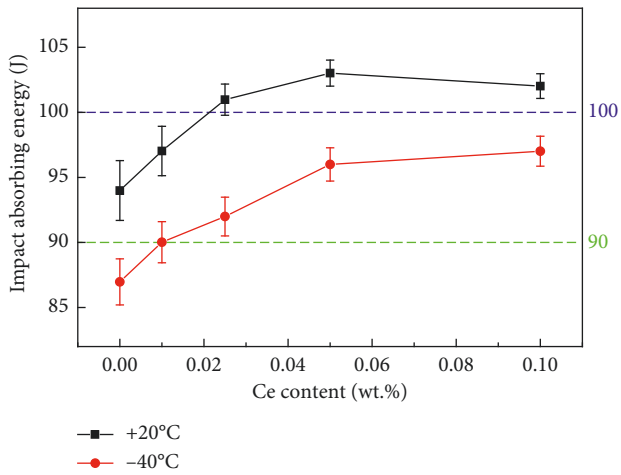

Figure 8: The evolutions of impact absorbing energy with the rare earth Ce content under different temperatures.

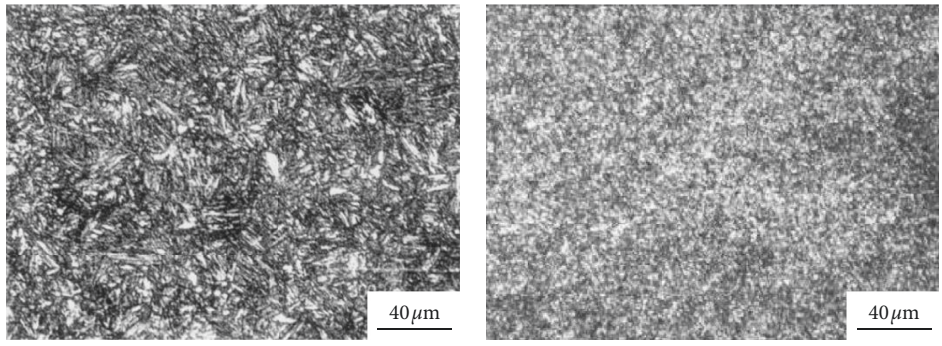

(a) (b)

Figure 9: The metallographs of 34CrNiMo6-0.05Ce specimens quenched in oil (870°C/30 min) and then tempered at 650°C: (a) as quenched in oil; (b) quenched and tempered.

contributes to improving strength and toughness. So, the 34CrNiMo6 steel could obtain good integrated mechanical properties after quenching process and tempering process.

To get a better understanding of the influencing mechanism of rare earth Ce content on the microstructures of 34CrNiMo6 steel, the micrographs of 34CrNiMo6 steel after quenching and QT at different temperatures from TEM are obtained and shown in Figure 10, respectively.

Lath martensite is usually massive and has nearly the same orientation, and the crystal with a shape like interconnected plates [18], which could be found in Figure 10(a). Moreover, the plate dimensions are limited by the dimensions of the austenite grain, which means that small martensite grains will give a fine needles structure. [18] This kind of structure has relatively desirable microstructure. The micrographs of 34CrNiMo6 steel with different rare earth Ce contents are shown in Figures 10(b) and 10(c), respectively. The microstructure is always tempered sorbite at the tempering temperatures used in this experiment. Generally, tempered sorbite is a mixture of the polygonal ferrite and relatively large cementite [19]. Compared with no addition of Ce, the spherification degree of cementite is more complete (Figure 10(c)) due to the higher content of Ce [20]. As the grain boundary could inhibit the movement of dislocation, the reduction of grain size can reduce the movement of dislocation, resulting in a significant effect on the mechanical properties [15]. Hence, the tensile of 34CrNiMo6-0.05Ce steel decreases compared with that of 34CrNiMo6-0Ce. In contrast, the toughness of 34CrNiMo6 steel will increase with the rare earth Ce content increasing due to the brittleness of cementite. The size of cementite has an effect on the mechanical behavior. Generally, the microstructure that consists of fine cementite is harder as well as stronger than that with coarse cementite, whereas coarse cementite is more ductile.

The TEM micrographs of 34CrNiMo6-xCe specimens quenched in oil (870°C/30 min) and tempered at tempered at 650°C are shown in Figure 11.

As mentioned before, the microstructure is tempered sorbite under the heat-treatment conditions at this experiment, which consist of the polygonal ferrite and cementite. The spherification degree of cementite is more complete with the rare earth Ce content increasing, resulting in the decrease of mechanical properties and improvement of ductility. This conclusion is consistent with the previous one.

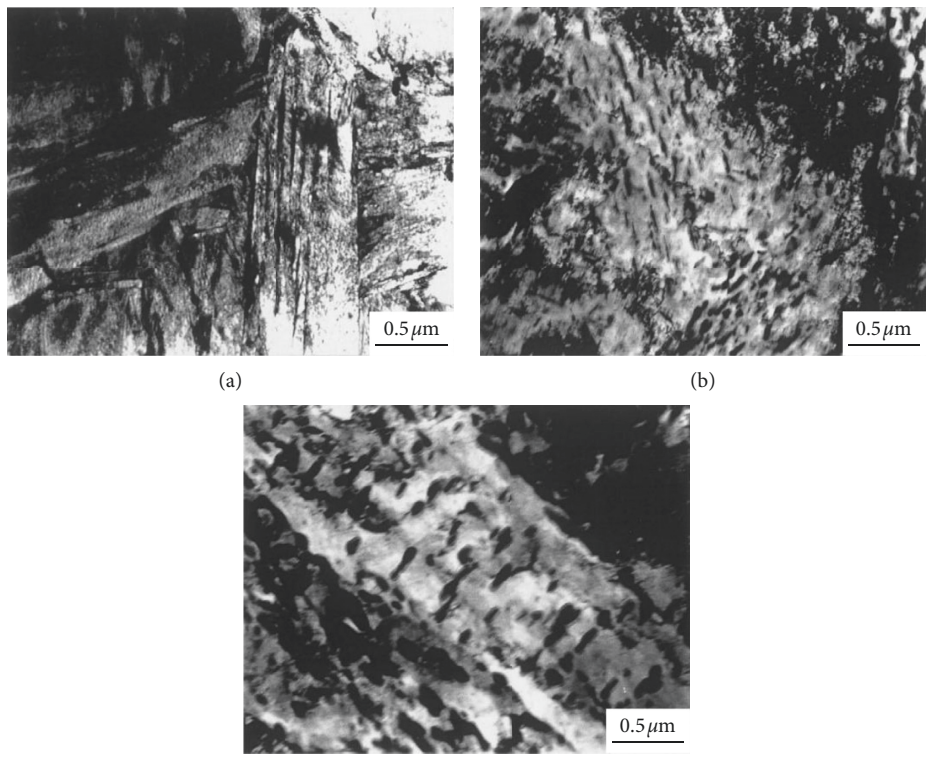

Figure 10: The TEM micrographs of 34CrNiMo6-xCe specimens quenched in oil (870°C/30 min) and tempered at 650°C: (a) $x = 0$, as quenched in oil; (b) $x = 0$, quenched and tempered; (c) $x = 0.05$, quenched and tempered.

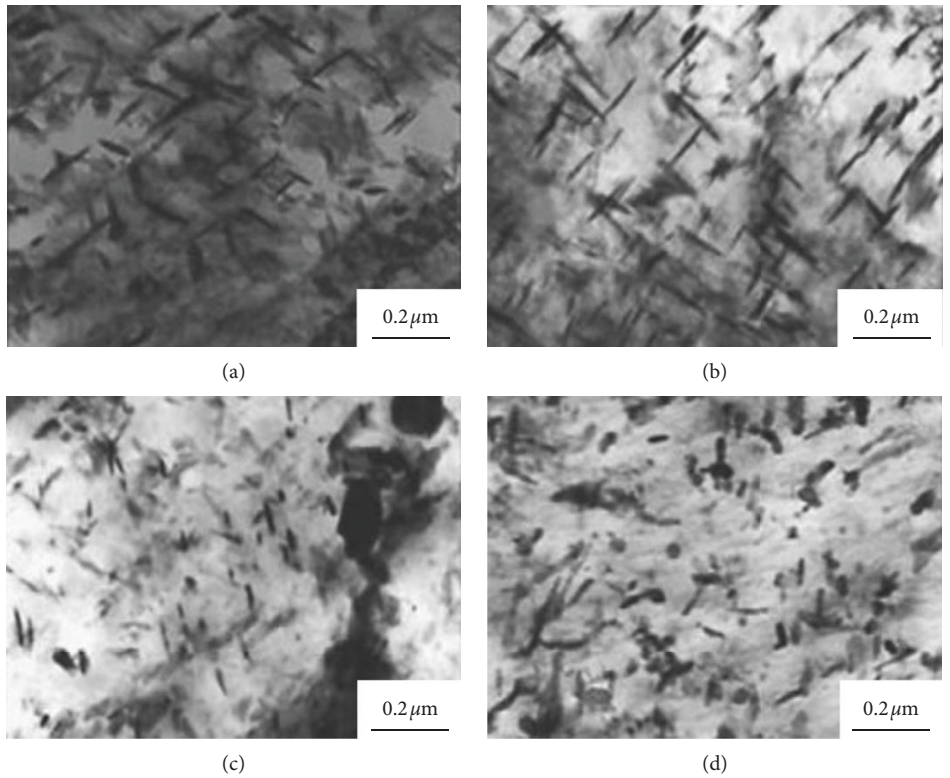

Figure 11: Fracture morphologies of 34CrNiMo6-xCe specimens quenched in oil (870°C/30 min) and tempered at 650°C: (a) $x = 0$, as quenched in oil; (b) $x = 0.025$, quenched and tempered; (c) $x = 0.05$, quenched and tempered; (d) $x = 0.1$, quenched and tempered.

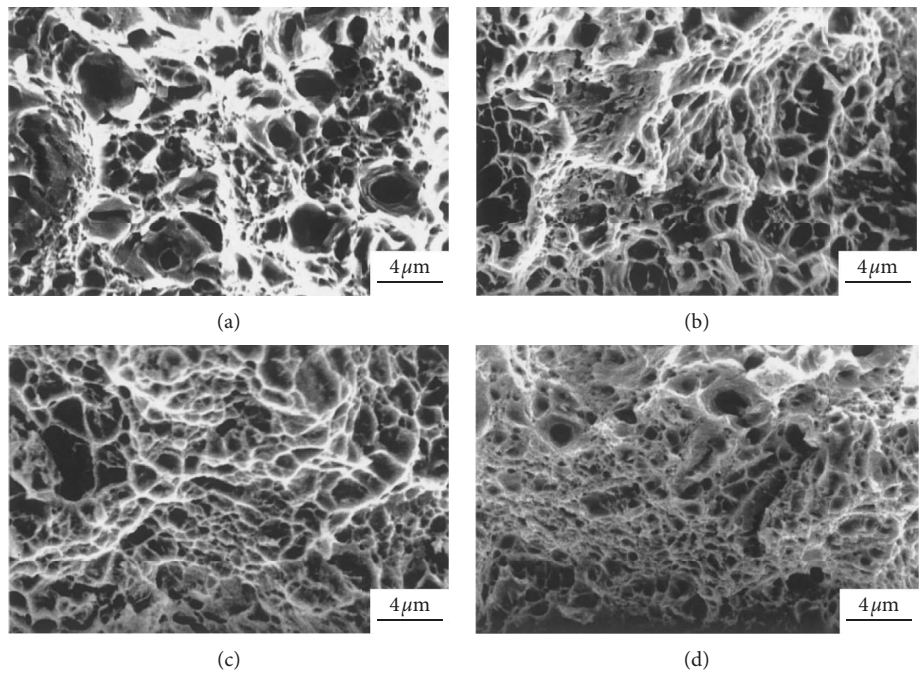

Figure 12: Fracture morphologies of 34CrNiMo6-xCe specimens quenched in oil (870°C/30 min) and tempered at 650°C: (a) $x = 0$, as quenched in oil (870°C/30 min), (b) $x = 0$, quenched and tempered, (c) $x = 0.025$, quenched and tempered, and (d) $x = 0.05$, quenched and tempered.

The fracture morphologies of specimens with different rare earth Ce contents quenched in oil and tempered are shown in Figure 12.

As shown in Figure 12, the fracture characteristic is always dominated by the ductile mechanism for all of the tempered specimens. The features observed from the micrographs are typical of most of the fracture surfaces under all the rare earth Ce contents. Moreover, the voids in these micrographs exhibit a fairly wide variation in size and shape, which could indicate that localized shear stresses may occur in addition to tensile stresses during the deformation process. It should be pointed out that although some voids existed in the fracture initiation area, there is no certain evidence proving that these voids were caused by the carbides.

4. Conclusions

The paper investigates the microstructure evolution during the heat treatment of 34CrNiMo6 steel by adjusting the rare earth Ce contents. In the experiments, five different rare earth Ce contents are adopted, respectively. The following conclusions can be drawn based on the experimental results:

(1) Both the tensile strength and yield strength decrease with the rare earth Ce content increasing. In contrast, the elongation after breakage increases with rare earth Ce content increasing before 0.05 wt.%, while remains almost stable from 0.05 wt.% to 0.1 wt.%. The Rockwell hardness C decreases with tempering temperature increasing before 0.05 wt.%, while keeps almost stable from 0.05 wt.% to 0.1 wt.%.

(2) The impact absorbing energy increases with rare earth Ce content increasing and then decreases from 0.05 wt.% to 0.1 wt.% when testing temperature is 20°C while increases monotonously with rare earth Ce content increasing when the testing temperature is −40°C.

(3) Based on the mechanical properties testing results under steady-state conditions and impact conditions and the related certification standard, it is highly recommended that the rare earth Ce content should be 0.025 wt.%–0.05 wt.%.

(4) The differences in mechanical properties among the different rare earth Ce contents may be the nucleation rate and growth of precipitates under different conditions. The spherification degree of cementite is more complete with rare earth Ce content, resulting in the decrease of mechanical properties and improvement of ductility.

(5) The fracture characteristic is always dominated by the ductile mechanism for all of the tempered specimens. The voids in the micrographs exhibit a fairly wide variation in size and shape, indicating that localized shear stresses may occur during the deformation process. Although some voids existed in the fracture initiation area, there is no certain evidence proving that these voids were caused by the carbides.

Data Availability

The data used to support the findings of this study are available from the corresponding author upon request.

Conflicts of Interest

The authors declare that there are no conflicts of interest regarding the publication of this paper.

Acknowledgments

This project was supported by the National Natural Science Foundation of China (grant no. 61727802) and National Defense Basic Scientific Research Project of China (grant no. JCKY2016208A001).

References

[1] M. R. Islam, S. Mekhilef, and R. Saidur, "Progress and recent trends of wind energy technology," *Renewable and Sustainable Energy Reviews*, vol. 21, pp. 456–468, 2013.

[2] F. Díaz-González, A. Sumper, O. Gomis-Bellmunt, and R. Villafáfila-Robles, "A review of energy storage technologies for wind power applications," *Renewable and Sustainable Energy Reviews*, vol. 16, no. 4, pp. 2154–2171, 2012.

[3] O. Ellabban, H. Abu-Rub, and F. Blaabjerg, "Renewable energy resources: current status, future prospects and their enabling technology," *Renewable and Sustainable Energy Reviews*, vol. 39, pp. 748–764, 2014.

[4] Q. Zhou, X. T. Xia, and Y. P. Zhang, "Optimal design of mainshaft bearing for wind turbine," *Advanced Materials Research*, vol. 171-172, pp. 252–255, 2011.

[5] M. Calcagnotto, D. Ponge, and D. Raabe, "Effect of grain refinement to 1μm on strength and toughness of dual-phase steels," *Materials Science and Engineering: A*, vol. 527, no. 29-30, pp. 7832–7840, 2010.

[6] H. Chunping, L. Xin, L. Fencheng, C. Jun, L. Fenggang, and H. Weidong, "Effects of cooling condition on microstructure and mechanical properties in laser rapid forming of 34CrNiMo6 thin-wall component," *The International Journal of Advanced Manufacturing Technology*, vol. 82, no. 5–8, pp. 1269–1279, 2016.

[7] W. Musial and J. Allread, "Test methodology and control of Full-Scale fatigue tests on wind turbine blades," *Wind Energy*, vol. 199, 1993.

[8] A. K. Belyaev, A. M. Polyanskiy, V. A. Polyanskiy, C. Sommitsch, and Y. A. Yakovlev, "Multichannel diffusion vs TDS model on example of energy spectra of bound hydrogen in 34CrNiMo6 steel after a typical heat treatment," *International Journal of Hydrogen Energy*, vol. 41, no. 20, pp. 8627–8634, 2016.

[9] N. Popescu, M. Cojocaru, and V. Mihailov, "Experimental studies on bulk tempering of 34CrNiMo6 steel," *Surface Engineering and Applied Electrochemistry*, vol. 48, no. 1, pp. 28–34, 2012.

[10] J. Cochet, S. Thuillier, T. Loulou, N. Decultot, P. Carré, and P.-Y. Manach, "Heat treatment of 34CrNiMo6 steel used for mooring shackles," *The International Journal of Advanced Manufacturing Technology*, vol. 91, no. 5–8, pp. 2329–2346, 2017.

[11] Z. Zhang, Z. Yin, T. Han, and A. C. C. Tan, "Fracture analysis of wind turbine main shaft," *Engineering Failure Analysis*, vol. 34, pp. 129–139, 2013.

[12] R. Wang, T. Han, W. Wang, Y. Xue, and D. Fu, "Fracture analysis and improvement of the main shaft of wind turbine based on finite element method," *Advances in Mechanical Engineering*, vol. 10, no. 4, 2018.

[13] H. D. Sun, K. Y. Zhao, J. Q. Rui et al., "Effect of tempering process on structure and properties of super martensitic stainless steel," *Advanced Materials Research*, vol. 581-582, pp. 1023–1026, 2012.

[14] D.-n. Zou, Y. Han, W. Zhang, and X.-d. Fang, "Influence of tempering process on mechanical properties of 00Cr13Ni4Mo supermartensitic stainless steel," *Journal of Iron and Steel Research International*, vol. 17, no. 8, pp. 50–54, 2010.

[15] A. Chatterjee, D. Chakrabarti, A. Moitra, R. Mitra, and A. K. Bhaduri, "Effect of normalization temperatures on ductile-brittle transition temperature of a modified 9Cr-1Mo steel," *Materials Science and Engineering: A*, vol. 618, pp. 219–231, 2014.

[16] C. Huang, X. Lin, F. Liu, H. Yang, and W. Huang, "High strength and ductility of 34CrNiMo6 steel produced by laser solid forming," *Journal of Materials Science and Technology*, vol. 35, no. 2, pp. 377–387, 2019.

[17] H. Muhammad Arslan and F. Ameeq, "Microstructural, mechanical and tribological investigation of 30CrMnSiNi2A ultra-high strength steel under various tempering temperatures," *Materials Research Express*, vol. 5, no. 1, article 016505, 2018.

[18] G. Miyamoto, N. Takayama, and T. Furuhara, "Accurate measurement of the orientation relationship of lath martensite and bainite by electron backscatter diffraction analysis," *Scripta Materialia*, vol. 60, no. 12, pp. 1113–1116, 2009.

[19] A. Shibata, F. Ichikawa, H. Adachi, T. Yamasaki, and N. Tsuji, "Cooperative strain accommodation over grains in martensitic transformation from Fe-Ni nanocrystalline austenite," *Philosophical Magazine Letters*, vol. 97, no. 4, pp. 132–139, 2017.

[20] N. V. Luzginova, L. Zhao, and J. Sietsma, "The cementite spheroidization process in high-carbon steels with different chromium contents," *Metallurgical and Materials Transactions A*, vol. 39, no. 3, pp. 513–521, 2008.